CellPress

Trends in Chemistry

Review

Taming radicals for stereoselective iron-catalyzed carbon–carbon bond formations

Lian-Jie Li (李连杰)[1], Dong-Song Zheng (郑冬松)[1,*], and Ze-Peng Yang (杨泽鹏)[1,*]

Stereoselective carbon–carbon (C–C) bond-forming reactions using Earth-abundant iron catalysts represent a significant challenge and opportunity in modern synthetic chemistry. While radical-mediated iron catalysis offers unique potential for the construction of molecular complexity, achieving high reactivity and stereoselectivity simultaneously is difficult due to the transient nature of radicals and the complicated electronic structure of iron. This review summarizes key advances from the past decade (2015–2025) in iron-catalyzed stereoselective C–C bond formations, organized around three emerging mechanistic paradigms: monoradical, dual-radical, and metalloradical pathways. Each paradigm is discussed with a focus on its unique reaction mechanisms, catalytic systems, and a range of applicable transformations, including cross-couplings, radical additions, radical–polar crossovers, and cyclopropanations. Finally, the future outlook of this field is discussed.

Highlights

Iron, the most abundant transition metal in the Earth's crust, stands out for its low toxicity, minimal environmental impact, and essential role in biological systems, making it a highly attractive candidate for sustainable catalysis.

Recent advances in stereoselective iron-catalyzed radical carbon–carbon bond formations have been organized around three emerging mechanistic paradigms: monoradical, dual-radical, and metalloradical pathways.

Iron's unique open-shell reactivity offers promising opportunities for constructing complex molecular architectures under mild and sustainable conditions, complementing traditional transition-metal catalysis.

The development of tailored ligand systems and multicatalytic platforms has enabled precise control over reactivity and stereoselectivity in iron-mediated radical transformations.

Stereoselective iron-catalyzed radical carbon–carbon bond formations

As the cornerstone of synthetic organic chemistry, carbon–carbon (C–C) bond formation enables the rapid assembly of complex molecular skeletons from simple building blocks, driving transformative progress in materials science and pharmaceutical chemistry. Among the strategies developed, transition metal-catalyzed C–C bond formations have emerged as a modular and versatile approach for the efficient construction of structurally complex carbon skeletons [1–3]. Based on the top 200 small-molecule drugs by retail sales in 2024, over half contain chiral C(sp^3) stereocenters (https://sites.arizona.edu/njardarson-lab/top200-posters/). To construct such three-dimensional frameworks, C–C bond formations involving C(sp^3) precursors have attracted considerable interest [4,5]. In this context, notable progress has been achieved through Earth-abundant metal-catalyzed C–C bond formations, particularly those facilitated by nickel, copper, and cobalt [6–15].

Despite notable progress with these metals, developing general and sustainable methods continues to drive the search for Earth-abundant alternatives. Iron, the most abundant transition metal in the Earth's crust, stands out for its low toxicity, minimal environmental impact, and indispensable role in biological processes, rendering it an especially attractive candidate for sustainable catalysis (Figure 1A) [16–18]. The history of iron-catalyzed C–C bond formations can be traced back to the 1940s [19], and the field attracted renewed attention in the 1970s when Kochi and coworkers demonstrated iron-catalyzed coupling reactions [20]. Since then, diverse iron-based catalytic systems have been introduced, in some cases achieving transformations that remain challenging for other metals [21–26]. Notably, a significant portion of these intriguing transformations proceeds via radical intermediates. While these open-shell species offer unique advantages, such as mild reaction conditions and broad functional group tolerance, the challenge lies in precisely harnessing and directing their reactivity with precision [27–30].

[1]Shanghai Key Laboratory of Chemical Assessment and Sustainability, School of Chemical Science and Engineering, Tongji University, Shanghai 200092, People's Republic of China

*Correspondence: zhengdongsong@tongji.edu.cn (D.-S. Zheng) and zpyang@tongji.edu.cn (Z.-P. Yang).

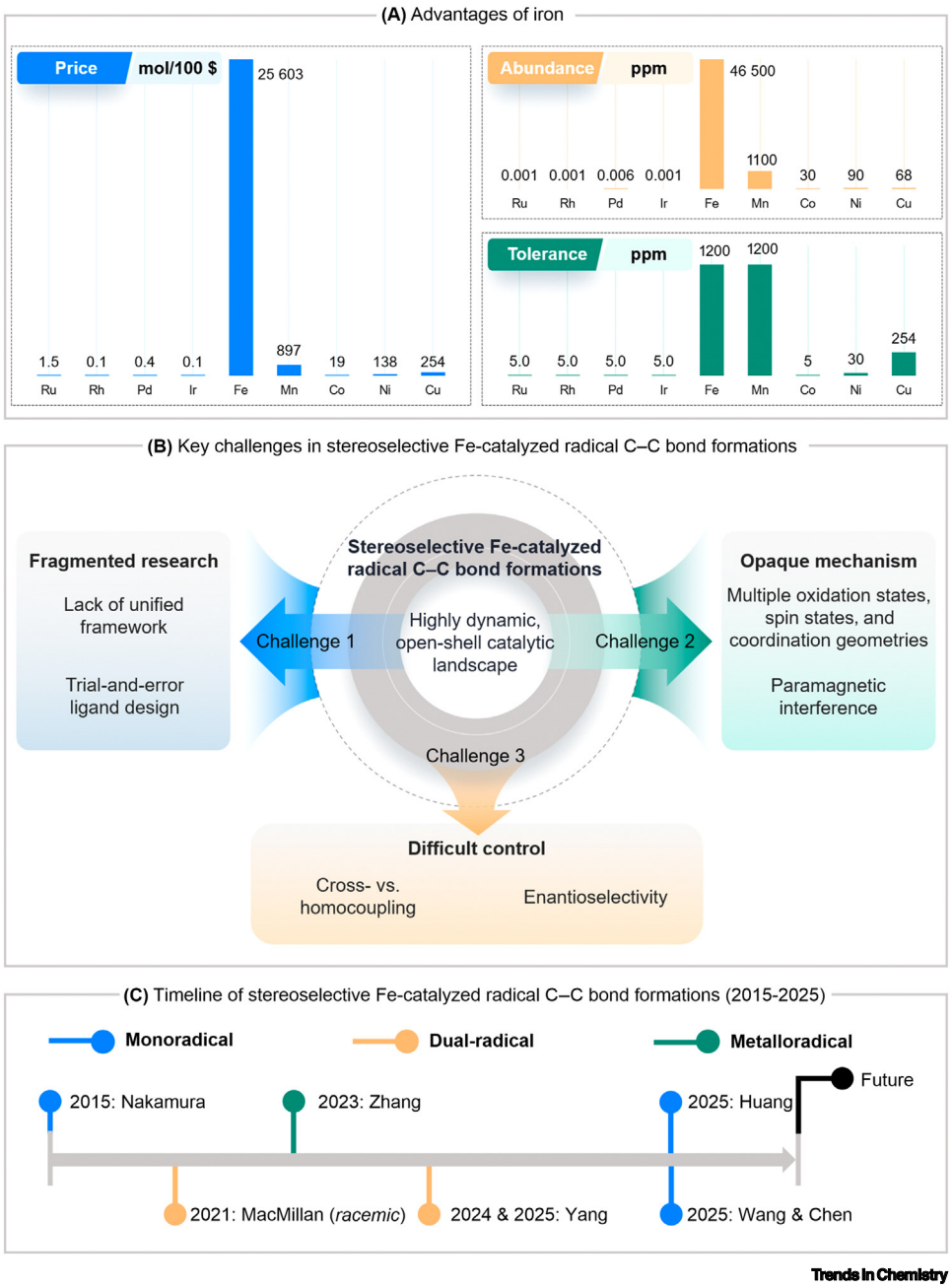

Figure 1. Background. A) Advantages of using iron as a sustainable catalyst to realize C–C formations (price comparison, natural abundance in the Earth's crust, and tolerance in drugs). (B) Key challenges in stereoselective Fe-catalyzed radical C–C bond formations. (C) Timeline of stereoselective Fe-catalyzed radical C–C bond formations. See [39,51,52,57,68,70,71,73,77].

Specifically, several key challenges have slowed the progress of iron-catalyzed radical C–C bond formations (Figure 1B), especially in achieving stereoselective reactions. First, research in this field remains fragmented. Many studies on iron catalysis are isolated cases, lacking a unified and comprehensive understanding. This issue is particularly evident in the underdevelopment of ligand systems. While effective ligand sets have been established for metals such as nickel and copper,

Glossary

Bimolecular homolytic substitution (S_H2): the radical counterpart to the S_N2 reaction, involving a concerted substitution where one radical replaces another on a substrate.
Electron paramagnetic resonance (EPR): a spectroscopy technique that detects samples with unpaired electrons by exposing them to microwave radiation in a magnetic field.
Halogen-atom transfer (XAT): a radical-initiation step in which a halogen atom is abstracted from an alkyl halide to generate a new radical intermediate.
Metalloradical catalysis (MRC): a catalytic process initiated by metal-centered radicals, which activate substrates homolytically to generate metal-entangled organic radicals that dictate the pathway and stereoselectivity of the transformation.
Outer-sphere: a reaction mode in which bond formation or electron transfer occurs between spatially separated species without direct coordination of the substrate to the metal center.
Radical–polar crossover (RPC): a mechanistic event wherein a radical intermediate is converted into an ionic species, enabling subsequent two-electron reaction pathway.
Radical sorting: a process by which different radical species are selectively discriminated and paired in a controlled manner, thereby enabling the formation of a desired cross-coupled product while suppressing undesired reactions such as homocoupling.
Single-electron transfer (SET): a fundamental process where one electron is moved from a donor species to an acceptor species.

selecting the appropriate ligand for iron catalysis still depends primarily on trial and error. Second, the fundamental mechanistic picture is complex [31–34]. The interplay between iron's multiple oxidation states, diverse spin states, and variable coordination geometries leads to a maze of possible reactive intermediates and pathways. The presence of paramagnetism and the uncertainty of the mechanisms make it challenging to identify the true active catalyst. As a result, there is limited guidance for the rational design of new reactions. Finally, precise control over selectivity is difficult. Radical couplings are often diffusion-controlled processes, which makes it hard to favor the desired cross-coupled products [35]. Moreover, managing the stereochemistry of these reactions adds another layer of complexity. The transient nature of radicals makes them difficult to tame, rendering the development of iron-catalyzed enantioselective C–C formations a frontier task.

Gratifyingly, the past decade (2015–2025) has witnessed groundbreaking progress in asymmetric iron-catalyzed radical C–C formations (Figure 1C). However, due to the inherent challenges of taming radicals and controlling stereoselectivity with iron, this area remained underexplored until recent years, particularly after 2023, when several pioneering asymmetric examples emerged and accelerated the field's development. Given iron's Earth-abundance, low toxicity, and unique ability to enable transformations that are difficult with other metals, this rapidly evolving area is poised to attract increasing attention. Yet, a systematic review that organizes and interprets these advances from a mechanistic perspective is still lacking. This article aims to fill this gap by offering a timely and structured overview centered on three emerging mechanistic paradigms: (i) monoradical pathway, (ii) dual-radical pathway, and (iii) metalloradical pathway. For clarity, this review does not cover oxidative or dehydrogenative couplings in which iron primarily acts as a Lewis acid [25]. These pathways have been successfully applied to a range of key transformations, including cross-couplings, radical additions, **radical–polar crossovers (RPC)** (see Glossary), and cyclopropanations. By categorizing the field according to distinct radical engagement modes, we provide both experts and non-specialists with a clear framework to understand the state of the art. For each paradigm, we highlight mechanistic principles, representative examples, and conceptual advances to inform the rational design of next-generation, highly efficient, and selective iron-catalyzed asymmetric radical processes.

Monoradical pathway

The monoradical pathway, as its name suggests, operates by generating a single alkyl radical species during the catalytic cycle. This approach, which is one of the earliest strategies developed, has proven to be effective in asymmetric cross-couplings by providing reliable control over the stereochemistry of transient, prochiral secondary radical intermediates. Recently, the monoradical method has been extended beyond cross-couplings to include other significant reactions, such as imine additions and radical-Mannich crossover reactions, highlighting its broader potential. In these systems, the key alkyl radical can be generated either through iron-mediated **single-electron transfer (SET)** processes from alkyl halides or through iron-independent pathways, such as **halogen-atom transfer (XAT)** processes.

In line with their longstanding research focus on achieving iron-catalyzed C–C bond formations [36–38], the Nakamura group reported the first iron-catalyzed enantioselective cross-coupling reaction in 2015 (Figure 2B, a) [39]. This landmark achievement was realized by a rigid P-chiral bisphosphine ligand that provides the necessary chiral environment to control the stereochemistry. In their subsequent mechanistic studies, the authors proposed a catalytic cycle involving the generation of a single alkyl radical (Figure 2A) [31]. The cycle begins with reduction of an alkyl halide by a chiral iron(I) species, generating a secondary alkyl radical while oxidizing the catalyst to an iron(II) intermediate. Following transmetalation with an organometallic reagent to form an

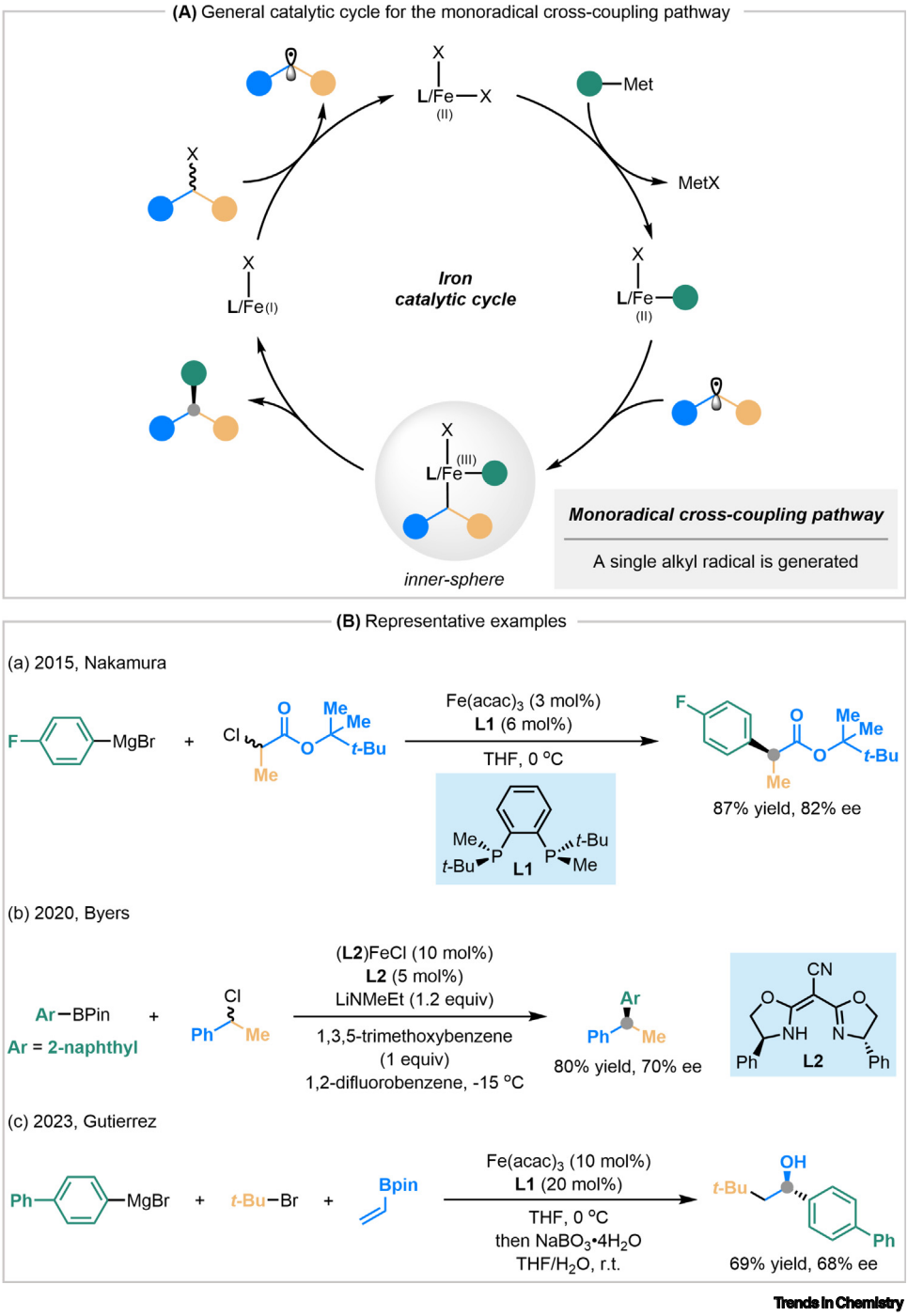

Figure 2. The monoradical cross-coupling pathway. (A) General catalytic cycle. (B) Representative examples. See [39,47,48]. Abbreviation: THF, tetrahedrofuran.

aryl–iron(II) complex, the key C–C bond formation proceeds via radical combination to yield an iron(III) species, which subsequently undergoes reductive elimination to release the enantioenriched coupling product and regenerate the active iron(I) catalyst. Notably, the C–C

bond formation follows an inner-sphere mechanism analogous to that observed in nickel-catalyzed radical cross-couplings [40–44], and the current system is, so far, limited to the construction of $C(sp^2)$–$C(sp^3)$ bonds.

By employing this method, a series of α-aryl esters are obtained in high yields with moderate-to-good enantioselectivity. Its synthetic utility is demonstrated by straightforward access to optically active ibuprofen and naproxen precursors. An interesting experimental observation is that the slow addition of the Grignard reagent is essential, as it significantly suppresses the formation of the diaryliron(II) intermediate, thereby minimizing the undesired homocoupling byproduct. This seminal study provides direct proof of concept that well-designed iron catalysts can effectively enforce stereochemical control in radical cross-coupling reactions.

Besides α-halo esters, other types of electrophiles have also been shown to be compatible with this type of transformation [45,46]. In 2020, Byers and coworkers reported an enantioselective iron-catalyzed Suzuki–Miyaura cross-coupling of benzylic halides with aryl boronic esters using a chiral cyanobis(oxazoline)–iron complex (Figure 2B, b) [47]. This protocol delivers enantioenriched 1,1-diarylalkanes, an important structural motif in pharmaceuticals, with excellent enantioselectivity. More recently, Gutierrez and coworkers described an iron-catalyzed multicomponent enantioselective cross-coupling in which vinyl boronates undergo dicarbofunctionalization with tertiary alkyl halides and aryl Grignard reagents (Figure 2B, c) [48]. In this system, the tertiary alkyl radical generated via iron(I)-mediated reduction of the alkyl halide is sterically hindered, preventing it from directly coupling with iron(II) species. Instead, it first adds to the alkene, producing a secondary alkyl radical that subsequently interacts with the aryl–iron(II) complex to deliver the multicomponent coupling product. This method achieves both high regio- and enantioselectivity, underscoring the potential of multicomponent radical reactions as an emerging frontier in asymmetric iron catalysis.

The ability of low-valent iron species to reductively activate alkyl halides, generating alkyl radicals via the SET process, provides a versatile platform for various radical-mediated transformations. This reactivity has been successfully extended to the radical addition to imines, establishing the reductive coupling of imines with alkyl electrophiles as a sustainable and powerful alternative to traditional nucleophilic additions [49,50]. Unlike conventional methods that rely on preformed organometallic reagents, this radical approach offers superior functional group tolerance and enables modular access to structurally diverse amine scaffolds, thereby expanding the synthetic toolbox for nitrogen-containing molecules. The stereochemical control in this transformation originates from a distinct mechanism where enantioselectivity is established during the radical addition to a coordinated imine, rather than through a radical combination/reductive elimination sequence (Figure 3A). The proposed catalytic cycle begins with the coordination of the imine substrate to a chiral low-valent Fe(I) complex. This key Fe(I) species then engages in an SET with an alkyl halide, generating an alkyl radical. The radical subsequently adds enantioselectively to the coordinated imine. Finally, protonation releases the chiral amine product, and a reduction step regenerates the Fe(I) catalyst.

This paradigm was realized by two independent reports in 2025, providing efficient methods for chiral α-tertiary amino acid derivatives. Wang and coworkers reported a system utilizing Fe(OTf) with a chiral bisoxazoline-phosphine (NPN) ligand and manganese powder as the reductant (Figure 3B, a) [51]. This protocol achieves excellent yields and enantioselectivity for both α-imino esters and α-imino amides, and the synthetic utility is further highlighted through late-stage functionalization of drug derivatives and the construction of nitrogen heterocycles bearing tetrasubstituted stereocenters. Mechanistic studies, including radical trapping experiments and **electron paramagnetic resonance (EPR)** spectroscopy, support the generation of alkyl

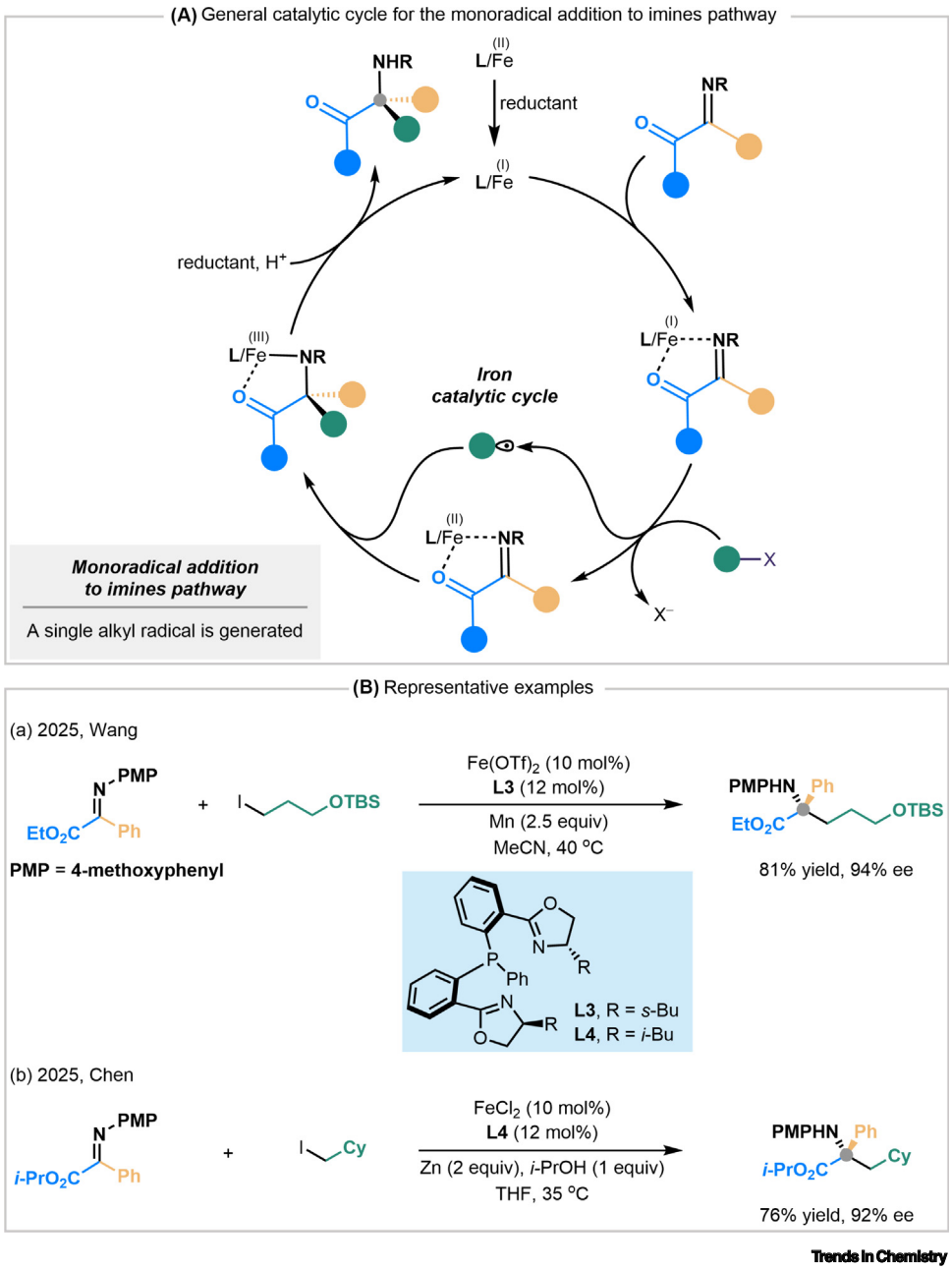

Figure 3. The monoradical addition to imines pathway. (A) General catalytic cycle. (B) Representative examples. See [51,52]. Abbreviations: PMP, 4-methoxyphenyl; TBS, *tert*-butyldimethylsilyl; Pr, propyl.

radical intermediates and the involvement of Fe(I) species in the catalytic cycle. Complementing this work, Chen and coworkers developed a similar reductive alkylation of α-imino esters employing a chiral NPN ligand (Figure 3B, b) [52]. This method delivers α-tertiary amino esters in high yields with excellent enantioselectivity, accommodating diverse primary, secondary, and tertiary alkyl iodides with broad functional group tolerance. In addition, the protocol can also be successfully extended to asymmetric benzylation using benzyl chlorides, yielding chiral phenylalanine derivatives with excellent enantioselectivity. Notably, both studies mark the pioneering use

of chiral NPN-type ligands in iron catalysis, providing a valuable reference for future ligand design in iron-catalyzed radical transformations.

RPC is a process in which a radical intermediate is captured by a transition metal through an SET and is then transformed into a polar species [53–56]. This change in mechanism enables the integration of the broad functional group tolerance found in radical pathways with the predictable stereocontrol and reactivity of two-electron ionic chemistry. By bridging one-electron and two-electron processes, RPC has expanded synthetic access to challenging bond formations between radical and polar synthons. Within this framework, a recent study by Huang and coworkers exemplifies an innovative monoradical Mannich crossover reaction for the synthesis of sterically hindered β-amino acid derivatives (Figure 4A) [57]. In this system, the reaction begins

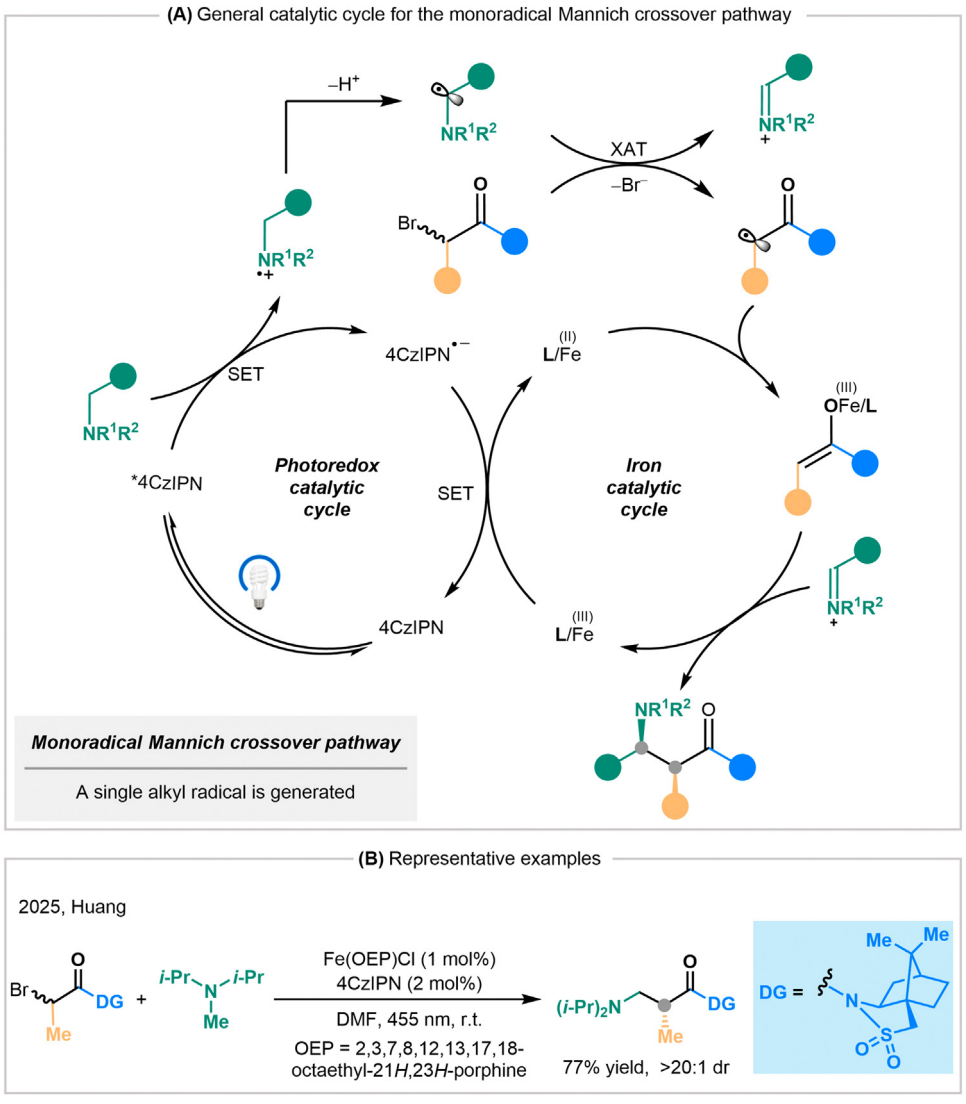

Figure 4. The monoradical Mannich crossover pathway. (A) General catalytic cycle. (B) Representative examples. See [57]. Abbreviations: XAT, halogen-atom transfer; 4CzIPN, 2,4,5,6-tetrakis(9-carbazolyl)isophthalonitrile; SET, single-electron transfer; OEP, 2,3,7,8,12,13,17,18-octaethyl-21*H*,23*H*-porphyrin; DG, directing group; DMF, *N*,*N*-dimethylformamide.

with the photoredox-induced oxidation of a tertiary amine to generate an α-amino alkyl radical. This radical then engages in an XAT with an α-bromo carbonyl compound, producing an α-carbonyl radical and an iminium ion pair. Next, rather than engaging in a sluggish radical addition, the α-carbonyl radical is captured by an iron catalyst to form a nucleophilic ferric enolate intermediate. This iron-stabilized enolate then participates in a Mannich-type addition with the iminium ion, forging the challenging C(sp^3)–C(sp^3) bond under mild conditions and with low catalyst loading (as low as 1 mol% Fe).

This system exhibits remarkable tolerance for sterically demanding substrates, enabling access to diverse β-amino acid derivatives. Notably, this platform can also be extended to α-trimethylsilyl (TMS)-substituted tertiary amines, which feature lower oxidation potentials and provide enhanced reactivity in the cross-coupling for certain substrates that show limited efficiency under standard conditions. In terms of stereocontrol, the reaction achieves excellent diastereoselectivity (>20:1 dr) using chiral auxiliaries such as Oppolzer's camphorsultam (Figure 4B). Efforts to implement a fully catalytic asymmetric variant using chiral iron complexes were also undertaken, yet resulted in limited enantioselectivity (≤37% ee), highlighting the challenge of achieving excellent stereocontrol by a chiral iron catalyst in this RPC manifold.

Dual-radical pathway

The dual-radical pathway represents a fundamentally distinct strategy in iron-catalyzed cross-couplings. This blueprint involves the generation of two radical species independently of the iron catalyst, enabling direct radical–radical cross-coupling [58–60]. This approach not only opens novel disconnection pathways but also serves as a powerful method for constructing challenging C(sp^3)–C(sp^3) bonds. A significant advantage of this paradigm is its ability to bypass the inherent functional group constraints, allowing diverse radical precursors, including carboxylic acids, halides, alcohols, and even carbon–hydrogen (C–H) compounds, to be coupled in virtually any combination, thus streamlining the synthesis of complex molecules from simple feedstocks [61–64]. However, achieving selective cross-coupling between two distinct transient radicals in a diffusion-controlled process is extremely difficult, and controlling enantioselectivity at newly formed stereocenters further compounds this problem [65–67]. Inspired by biomimetic principles, an iron-catalyzed strategy has recently been developed to address this issue through a **bimolecular homolytic substitution (S_H2)** mechanism that ensures effective **radical sorting** (Figure 5A) [68]. In this system, a low-valent iron complex preferentially captures a less sterically hindered primary alkyl radical, forming a relatively stable iron–alkyl intermediate. The second radical, typically a more sterically demanding secondary or tertiary alkyl radical, then reacts with the iron–alkyl species via an **outer-sphere** pathway. The distinct steric hindrance between the two types of radicals ensures efficient differentiation and sequential coupling, thereby achieving high cross-selectivity for iron-catalyzed radical–radical cross-couplings [69].

In 2021, MacMillan and coworkers pioneered this strategy in C(sp^3)–C(sp^3) cross-couplings using a dual photoredox/iron catalytic system (Figure 5B, a). This work successfully translates the S_H2 mechanism, a paradigm well-established in enzymatic alkylation pathways, such as those involving methylcobalamin [70], into a general synthetic platform. By leveraging an iron porphyrin catalyst, the system initially captures a primary alkyl radical to form an organo-iron intermediate, which subsequently acts as a radical acceptor for a more sterically hindered radical species. This mechanism elegantly partitions the roles of the two distinct radicals, thereby solving the central challenge of cross-selectivity in radical–radical cross-couplings by suppressing the homocoupling between radicals of the same type. This platform shows considerable generality, successfully achieving not only primary/tertiary but also primary/secondary radical–radical cross-couplings, providing a versatile route to access compounds bearing quaternary or tertiary stereocenters. Nevertheless, these transformations occur in a racemic/achiral fashion, although

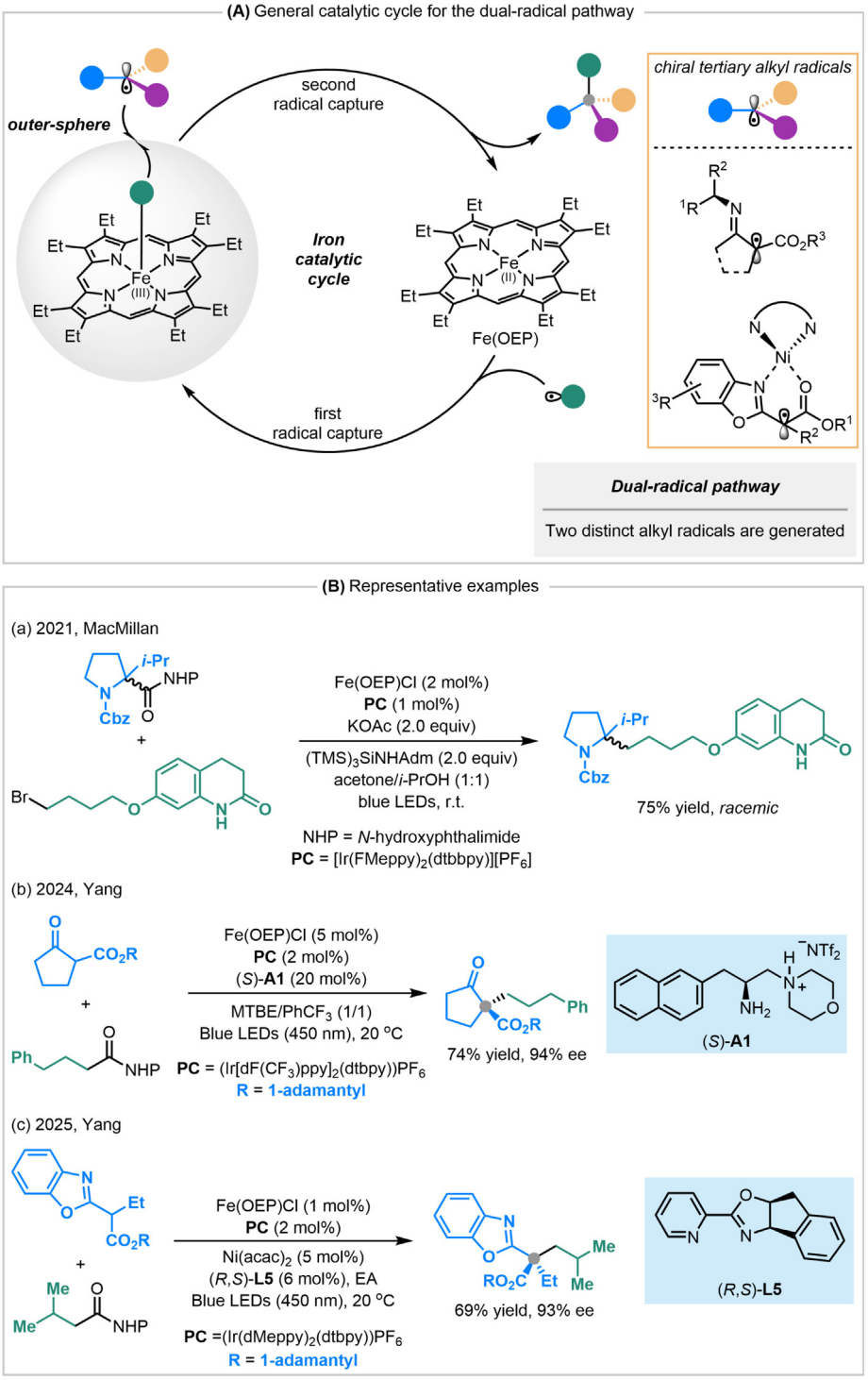

Figure 5. The dual-radical pathway. (A) General catalytic cycle. (B) Representative examples. See [70,71,73]. Abbreviations: TMS, trimethylsilyl; SiNHAdm, silylated derivative of amantadine; OEP, 2,3,7,8.12,13,17,18-octaethyl-21*H*,23*H*-porphyrin; PC, photocatalyst; NHP, *N*-hydroxyphthalimide; MTBE: methyl *tert*-butyl ether; $PhCF_3$, trifluoromethylbenzene; KOAc: potassium acetate.

the iron porphyrin catalyst exhibits a certain degree of diastereocontrol in specific cases. The outer-sphere mechanism, while enabling efficient C–C bond formation distal to the metal center, simultaneously constrains stereochemical influence from the catalyst's chiral environment. This spatial separation between the chiral metal catalyst and the reaction site poses a fundamental obstacle to achieving consistently good enantiocontrol.

This challenge has been partially addressed by the Yang group through a sophisticated cooperative catalysis strategy. In 2024, they established a platform that successfully merges photoredox, iron, and chiral primary amine catalysis to achieve the highly enantioselective construction of cyclic quaternary stereocenters via a radical-based, outer-sphere cross-coupling mechanism (Figure 5B, b) [71]. This triple-catalysis system effectively divides the tasks of the catalytic cycles. The photoredox system produces both primary alkyl radicals from NHP (*N*-hydroxyphthalimide) esters and enaminyl radicals through oxidation, while the iron porphyrin serves as a selective catalyst to sort primary and tertiary radical species. Meanwhile, the chiral primary amine catalyst plays the crucial stereochemical role by condensing with 1,3-dicarbonyl compounds to form chiral enamines, which, upon oxidation, generate chiral enaminyl radicals [72]. These preorganized chiral radicals then serve as stereodefined coupling partners in the subsequent bond-forming step. The system shows good generality, accommodating a wide range of unactivated alkyl NHP esters and cyclic 1,3-dicarbonyl compounds under mild, base-free conditions. However, when acyclic substrates are employed, the yield is notably low, even after extending the reaction time to 3 days (31–34% yields), although the enantioselectivity is still promising (87–96% ee).

Building on this success, the Yang group further advanced the field in 2025 by tackling the challenge of constructing quaternary stereocenters in acyclic frameworks (Figure 5B, c) [73]. They realized this goal through a new synergistic system comprising photoredox, iron, and a chiral Lewis acid catalyst. In this system, the chiral Lewis acid is proposed to bind to the substrate, creating a well-defined chiral environment that governs the stereochemistry of the key radical intermediate. This work significantly expands the scope of accessible molecular architectures, moving beyond cyclic constraints to valuable acyclic motifs.

Metalloradical pathway

The metalloradical pathway represents a novel paradigm for asymmetric iron-catalyzed C–C bond formations. **Metalloradical catalysis (MRC)** exploits metal-centered radicals in open-shell complexes to generate metal-stabilized organic radicals, which serve as key intermediates governing subsequent homolytic reactions [74–76]. As a proof of concept, this principle has been successfully applied to the iron-catalyzed asymmetric cyclopropanations of alkenes using *in situ* generated diazo compounds by the Zhang group (Figure 6A) [77]. The catalytic cycle operates through a sequence of three critical steps. First, metalloradical activation occurs as the Fe(III) catalyst homolytically activates the diazo reagent, extruding N and generating a metal-stabilized α-Fe(IV)-alkyl radical intermediate. Next, this carbon-centered radical adds across the alkene π-bond in a radical addition step, forming a γ-Fe(IV)-alkyl radical. Finally, intramolecular radical substitution takes place via a 3-exo-tet cyclization, ring-closing to deliver the cyclopropane product while regenerating the Fe(III) metalloradical catalyst. This stepwise radical mechanism is robustly supported by a combination of experimental and computational evidence.

Supported by a D -symmetric chiral amidoporphyrin ligand, this Fe(III)-based MRC system achieves excellent enantioselectivity and high diastereoselectivity for a broad range of alkenes, providing efficient access to valuable trifluoromethyl-substituted cyclopropanes (Figure 6B). Beyond standard styrenes, the protocol accommodates substrates bearing electron-donating

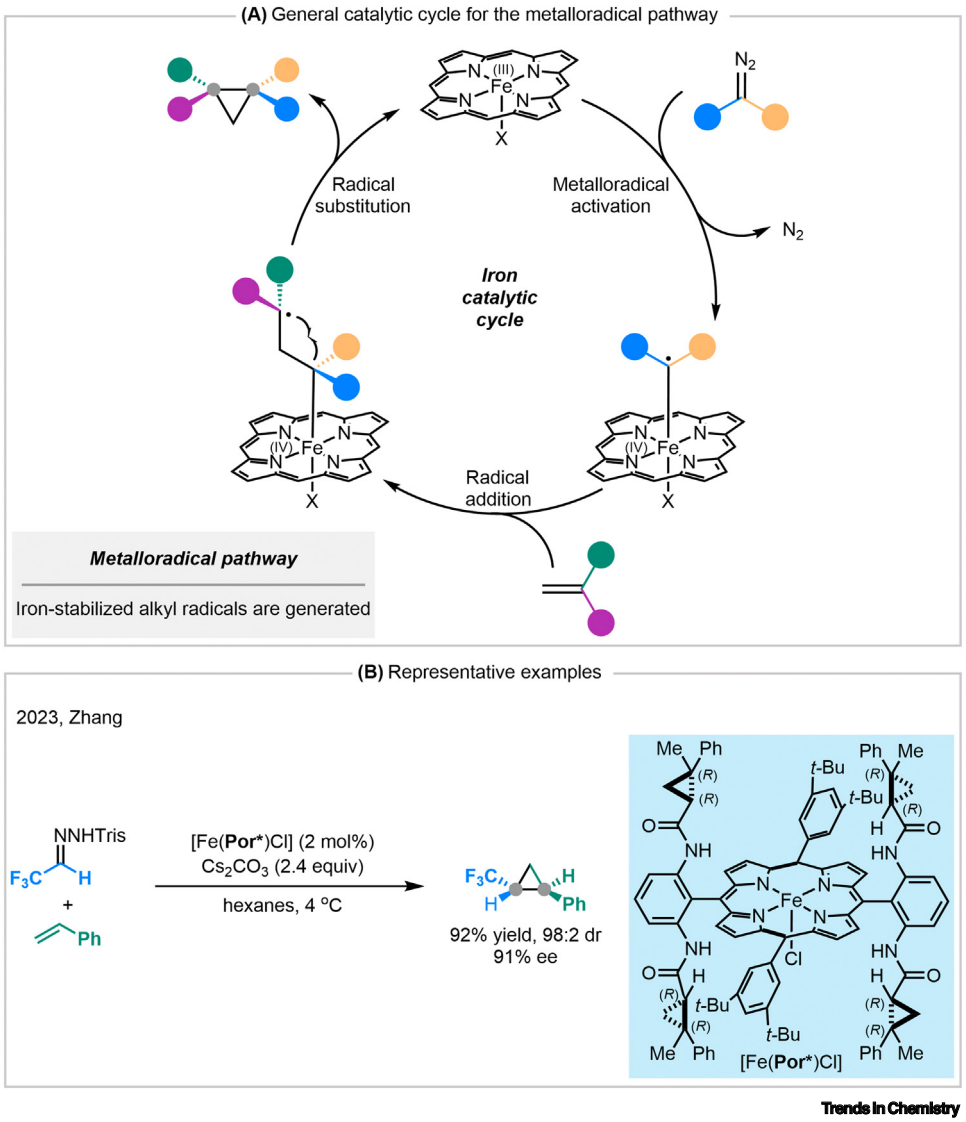

Figure 6. The metalloradical pathway. (A) General catalytic cycle. (B) Representative examples. See [77].

and electron-withdrawing substituents, all with high efficiency. In addition, it successfully tackles certain 1,1-disubstituted alkenes, enabling the stereoselective construction of cyclopropanes featuring all-carbon quaternary stereocenters and complex spirocyclic architectures. Furthermore, the system's generality is proven by its competence with an array of diazo precursors. The broad scope, combined with operational simplicity and high stereocontrol, underscores its significant synthetic value.

Concluding remarks

Over the past decade, the field of stereoselective iron-catalyzed radical C–C bond formations has evolved from a conceptual challenge into a dynamically advancing area of synthetic chemistry. As summarized in this review, three distinct yet complementary mechanistic paradigms, including monoradical, dual-radical, and metalloradical pathways, have emerged as powerful strategies to address the issues of reactivity and selectivity in iron-mediated transformations. These

Outstanding questions

Can chiral iron complexes be developed to replace stoichiometric chiral auxiliaries in radical–polar crossover reactions for practical asymmetric synthesis?

How can iron-catalyzed dual-radical strategies be engineered to construct congested $C(sp^3)$–$C(sp^3)$ bonds between two sterically demanding secondary or tertiary radicals while controlling the configuration of multiple stereocenters?

Can metalloradical catalysis be effectively extended beyond cyclopropanation to other key carbon–carbon (C–C) bond-forming radical transformations, including enantioselective carbon–hydrogen alkylation?

Can we establish a predictive model that correlates iron's ligand field, its open-shell electronic structure, and the resulting stereochemical outcome to guide the rational design of next-generation catalysts?

Can the merger of iron catalysis with photoredox or electrocatalysis enable new, stereoselective C–C bond-forming reactions that are currently beyond the reach of nickel or copper catalysis?

Can the application of methods like ultrafast spectroscopy directly identify and characterize the key iron intermediates proposed in these radical mechanisms to guide rational catalyst design?

Can these iron-catalyzed radical couplings directly generate novel three-dimensional scaffolds for pharmaceutical lead optimization?

approaches have enabled a range of previously challenging asymmetric transformations under mild and sustainable conditions. Key to this progress has been the design of tailored ligand systems and multi-catalytic platforms that effectively manage radical intermediates and enforce stereocontrol.

Despite these impressive advances, significant challenges and limitations persist (see Outstanding questions). The monoradical cross-coupling pathway is fundamentally important but is currently limited to specific classes of substrates. Additionally, it has not yet produced applicable methods for challenging $C(sp^3)$–$C(sp^3)$ couplings. This approach also struggles with stereochemical control, as there are few examples that achieve high enantioselectivity (≥90% ee). This situation underscores the ongoing need for enhanced chiral induction systems. The dual-radical strategy represents a significant shift in addressing the challenges associated with forming quaternary carbon centers. However, it relies on the inherent stereochemistry of the chiral tertiary radical generated *in situ* instead of using catalyst-controlled enantioselection. Moreover, the range of compatible radical partners is quite limited, primarily restricted to primary/tertiary alkyl radicals, which significantly limits the method's synthetic versatility. Therefore, there is a critical need to develop versatile ligand frameworks that can provide stereocontrol directly at the iron center while accommodating a wider variety of radical precursors. Although the metalloradical pathway has demonstrated exceptional stereocontrol in cyclopropanation reactions, its application scope remains narrow. The potential of this platform for other important transformations, such as stereocontrolled C–H insertion or other carbene transfer reactions, remains largely unexplored. The stepwise radical mechanism intrinsic to the metalloradical pathway may unlock reactivity and stereocontrol distinct from traditional metal-carbene chemistry, thereby enabling the synthesis of challenging molecular frameworks previously inaccessible through conventional strategies.

Looking forward, several exciting directions remain open for exploration. First, ligand design represents a central bottleneck in stereoselective iron catalysis, as it should simultaneously address multiple requirements rather than following a single linear trajectory. As a relatively hard, early transition metal, iron requires ligand frameworks that maintain catalytic activity by stabilizing open-shell intermediates while accommodating frequent single-electron events. Accordingly, effective ligand systems are typically dominated by hard donor atoms, especially nitrogen or oxygen donors, to better match iron's electronic profile. Moreover, iron's propensity for high coordination numbers, often approaching six-coordination, means that stereochemical control also depends on the ligand's ability to occupy and organize multiple coordination sites, thereby enforcing compact and well-defined transition states. Tridentate, tetradentate, and pentadentate ligand frameworks are therefore especially valuable. In addition, it is important to strategically incorporate secondary weak interactions, such as hydrogen bonding or π-stacking, to create well-defined chiral binding pockets that guide substrate orientation. Taken together, this integrated design philosophy draws inspiration from enzymatic systems, with the goal of developing simpler, synthetically accessible iron catalysts that retain, and potentially extend, the reactivity and selectivity profiles of native iron enzymes. In addition, expanding the range of compatible cooperative chiral controllers, such as hydrogen-bonding catalysts, chiral anions, or engineered metalloenzymes, may also broaden these systems.

Second, significantly expanding the substrate scope is necessary to improve the generality and applicability of iron-catalyzed methods. Future efforts should unlock new reactivity and selectivity, particularly for challenging substrates, including unactivated alkyl electrophiles, acyclic precursors, and more demanding coupling partners, such as secondary/secondary, secondary/tertiary, and tertiary/tertiary alkyl systems. Integration with enabling technologies, such as photoredox

catalysis and electrocatalysis, could be crucial to accelerate the development of practical and scalable iron-catalyzed systems.

Third, to further advance this promising research area, establishing a much higher standard for in-depth mechanistic investigation will be essential for the field's long-term success. Rigorous mechanistic studies should become a defining expectation for radical-based catalytic systems, enabling researchers to distinguish between stepwise radical pathways and superficially similar two-electron mechanisms. Among the suite of available mechanistic tools, EPR spectroscopy stands out as uniquely powerful and indispensable for probing transient organic radicals and metalloradical intermediates, offering direct insight into electronic structures, spin distributions, and the identities of key radical species. Complementary techniques, such as ultrafast spectroscopy, Mössbauer spectroscopy, and additional advanced physical methods, will further help elucidate reaction pathways and selectivity-determining steps. Such fundamental understanding should guide rational ligand design, clarify the origins of reactivity and stereoselectivity, and ultimately enable the development of more versatile and broadly applicable iron-based catalytic radical systems.

As iron continues to serve as an Earth-abundant and biologically relevant alternative to precious metals, we anticipate that its unique open-shell reactivity will inspire increasingly creative solutions to selectivity challenges. Such advances will not only enable new disconnections in complex molecule synthesis but also contribute meaningfully to the development of sustainable and selective methodologies for C–C bond formation.

Acknowledgments

Support has been provided by the National Natural Science Foundation of China (Grant no. 22201216 to Z-P.Y.), the National Key Research & Development Program of China (Grant no. 2023YFA1508600 to Z-P.Y.), and the Fundamental Research Funds for the Central Universities (Grant no. 22120240079 to Z-P.Y.).

Declaration of interests

The authors declare no competing interests.

References

1. de Meijere, A. *et al.* (2014) *Metal-Catalyzed Cross-Coupling Reactions and More*, Wiley
2. Jana, R. *et al.* (2011) Advances in transition metal (Pd,Ni,Fe)-catalyzed cross-coupling reactions using alkyl-organometallics as reaction partners. *Chem. Rev.* 111, 1417–1492
3. Johansson Seechurn, C.C.C. *et al.* (2012) Palladium-catalyzed cross-coupling: a historical contextual perspective to the 2010 Nobel Prize. *Angew. Chem. Int. Ed.* 51, 5062–5085
4. Choi, J. and Fu, G.C. (2017) Transition metal–catalyzed alkyl-alkyl bond formation: another dimension in cross-coupling chemistry. *Science* 356, eaaf7230
5. Fu, G.C. (2017) Transition-metal catalysis of nucleophilic substitution reactions: a radical alternative to S_N1 and S_N2 processes. *ACS Cent. Sci.* 3, 692–700
6. Cherney, A.H. *et al.* (2015) Enantioselective and enantiospecific transition-metal-catalyzed cross-coupling reactions of organometallic reagents to construct C–C bonds. *Chem. Rev.* 115, 9587–9652
7. Xue, W. *et al.* (2021) Nickel-catalyzed formation of quaternary carbon centers using tertiary alkyl electrophiles. *Chem. Soc. Rev.* 50, 4162–4184
8. Ehehalt, L.E. *et al.* (2024) Cross-electrophile coupling: principles, methods, and applications in synthesis. *Chem. Rev.* 124, 13397–13569
9. You, L.-X. *et al.* (2025) Ni-catalyzed cross-electrophile alkyl-alkyl coupling reactions. *Sci. China Chem.* 68, 3376–3400
10. Gu, Q.-S. *et al.* (2020) Copper(I)-catalyzed asymmetric reactions involving radicals. *Acc. Chem. Res.* 53, 170–181
11. Wang, P.-Z. *et al.* (2024) Photocatalysis meets copper catalysis: a new opportunity for asymmetric multicomponent radical cross-coupling reactions. *Acc. Chem. Res.* 57, 3433–3448
12. Cahiez, G. and Moyeux, A. (2010) Cobalt-catalyzed cross-coupling reactions. *Chem. Rev.* 110, 1435–1462
13. Hammann, J.M. *et al.* (2017) Recent advances in cobalt-catalyzed Csp^2 and Csp^3 cross-couplings. *Synthesis* 49, 3887–3894
14. Zhang, Z. *et al.* (2022) Copper-catalyzed radical relay in $C(sp^3)$–H functionalization. *Chem. Soc. Rev.* 51, 1640–1658
15. Zhu, N. *et al.* (2024) Metal-catalyzed asymmetric reactions enabled by organic peroxides. *Chem. Soc. Rev.* 53, 2326–2349
16. Morgan, J.W. *et al.* (1980) Chemical composition of Earth, Venus, and Mercury. *Proc. Natl. Acad. Sci. U. S. A.* 77, 6973–6977
17. Tchounwou, P.B. *et al.* (2012) Heavy metal toxicity and the environment. In *Molecular, Clinical and Environmental Toxicology* (Luch, A., ed.), pp. 133–164, Springer Basel
18. Gandeepan, P. *et al.* (2019) 3d Transition metals for C–H activation. *Chem. Rev.* 119, 2192–2452
19. Kharasch, M.S. and Fields, E.K. (1941) Factors determining the course and mechanisms of Grignard reactions. IV. The effect of metallic halides on the reaction of aryl Grignard reagents and organic halides. *J. Am. Chem. Soc.* 63, 2316–2320
20. Tamura, M. and Kochi, J.K. (1971) Vinylation of Grignard reagents. Catalysis by iron. *J. Am. Chem. Soc.* 93, 1487–1489
21. Bolm, C. *et al.* (2004) Iron-catalyzed reactions in organic synthesis. *Chem. Rev.* 104, 6217–6254

22. Sherry, B.D. and Fürstner, A. (2008) The promise and challenge of iron-catalyzed cross coupling. *Acc. Chem. Res.* 41, 1500–1511
23. Bauer, I. and Knölker, H.-J. (2015) Iron catalysis in organic synthesis. *Chem. Rev.* 115, 3170–3387
24. Piontek, A. *et al.* (2018) Iron-catalyzed cross-couplings in the synthesis of pharmaceuticals: in pursuit of sustainability. *Angew. Chem. Int. Ed.* 57, 11116–11128
25. Zhang, J. and Wu, J. (2024) Recent progress in asymmetric radical reactions enabled by chiral iron catalysts. *Chem. Commun.* 60, 12633–12649
26. Li, L.-J. *et al.* (2024) Recent advances in Mn, Fe, Co, and Ni-catalyzed organic reactions. *CCS Chem.* 6, 537–584
27. Studer, A. and Curran, D.P. (2016) Catalysis of radical reactions: a radical chemistry perspective. *Angew. Chem. Int. Ed.* 55, 58–102
28. Smith, J.M. *et al.* (2018) Radical retrosynthesis. *Acc. Chem. Res.* 51, 1807–1817
29. Chan, A.Y. *et al.* (2022) Metallaphotoredox: the merger of photoredox and transition metal catalysis. *Chem. Rev.* 122, 1485–1542
30. Huang, C.-Y. *et al.* (2022) Photocatalytic C(sp^3) radical generation *via* C–H, C–C, and C–X bond cleavage. *Chem. Sci.* 13, 5465–5504
31. Sharma, A.K. *et al.* (2017) DFT and AFIR study on the mechanism and the origin of enantioselectivity in iron-catalyzed cross-coupling reactions. *J. Am. Chem. Soc.* 139, 16117–16125
32. Lee, W. *et al.* (2017) Mechanism of Nakamura's bisphosphine-iron-catalyzed asymmetric C(sp^2)–C(sp^3) cross-coupling reaction: the role of spin in controlling arylation pathways. *J. Am. Chem. Soc.* 139, 16126–16133
33. Sears, J.D. *et al.* (2018) Intermediates and mechanism in iron-catalyzed cross-coupling. *J. Am. Chem. Soc.* 140, 11872–11883
34. Zhang, B. *et al.* (2022) 7.04—Recent advances in synthesis, characterization and reactivities of iron-alkyl and iron-aryl complexes. In *Comprehensive Organometallic Chemistry IV* (7), pp. 185–209
35. Leifert, D. *et al.* (2020) The persistent radical effect in organic synthesis. *Angew. Chem. Int. Ed.* 59, 74–108
36. Nakamura, M. *et al.* (2004) Iron-catalyzed cross-coupling of primary and secondary alkyl halides with aryl Grignard reagents. *J. Am. Chem. Soc.* 126, 3686–3687
37. Hatakeyama, T. *et al.* (2010) Iron-catalyzed Suzuki–Miyaura coupling of alkyl halides. *J. Am. Chem. Soc.* 132, 10674–10676
38. Hatakeyama, T. *et al.* (2011) Tuning chemoselectivity in iron-catalyzed Sonogashira-type reactions using a bisphosphine ligand with peripheral steric bulk: selective alkynylation of nonactivated alkyl halides. *Angew. Chem. Int. Ed.* 50, 10973–10976
39. Jin, M. *et al.* (2015) Iron-catalyzed enantioselective cross-coupling reactions of α-chloroesters with aryl Grignard reagents. *J. Am. Chem. Soc.* 137, 7128–7134
40. Schley, N.D. and Fu, G.C. (2014) Nickel-catalyzed Negishi arylations of propargylic bromides: a mechanistic investigation. *J. Am. Chem. Soc.* 136, 16588–16593
41. Yin, H. and Fu, G.C. (2019) Mechanistic investigation of enantioconvergent Kumada reactions of racemic α-bromoketones catalyzed by a nickel/bis(oxazoline) complex. *J. Am. Chem. Soc.* 141, 15433–15440
42. Yuan, M. *et al.* (2020) On the nature of C(sp^3)–C(sp^2) bond formation in nickel-catalyzed tertiary radical cross-couplings: a case study of Ni/photoredox catalytic cross-coupling of alkyl radicals and aryl halides. *J. Am. Chem. Soc.* 142, 7225–7234
43. Dawson, G.A. *et al.* (2023) Nickel-catalyzed radical mechanisms: informing cross-coupling for synthesizing non-canonical biomolecules. *Acc. Chem. Res.* 56, 3640–3653
44. Spielvogel, E.H. *et al.* (2025) Nickel-mediated radical capture: evidence for a concerted inner-sphere mechanism. *J. Am. Chem. Soc.* 147, 19632–19642
45. Iwamoto, T. *et al.* (2019) Iron-catalysed enantioselective Suzuki–Miyaura coupling of racemic alkyl bromides. *Chem. Commun.* 55, 1128–1131
46. Liu, L. *et al.* (2020) Intra- and intermolecular Fe-catalyzed dicarbofunctionalization of vinyl cyclopropanes. *Chem. Sci.* 11, 3146–3151
47. Tyrol, C.C. *et al.* (2020) Iron-catalysed enantioconvergent Suzuki–Miyaura cross-coupling to afford enantioenriched 1,1-diarylalkanes. *Chem. Commun.* 56, 14661–14664
48. Youshaw, C.R. *et al.* (2023) Iron-catalyzed enantioselective multicomponent cross-couplings of α-boryl radicals. *Org. Lett.* 25, 8320–8325
49. Zhang, C. *et al.* (2024) A general enantioselective α-alkyl amino acid derivatives synthesis enabled by cobalt-catalyzed reductive addition. *J. Am. Chem. Soc.* 146, 25918–25926
50. Wu, X. *et al.* (2024) Modular α-tertiary amino ester synthesis through cobalt-catalysed asymmetric aza-Barbier reaction. *Nat. Chem.* 16, 398–407
51. Wang, J. *et al.* (2025) Iron-catalyzed asymmetric reductive cross-coupling of ketimines with alkyl iodides. *J. Am. Chem. Soc.* 147, 29666–29672
52. Bai, J. *et al.* (2025) Iron-catalyzed asymmetric cross-electrophile alkylation of imines. *ACS Catal.* 15, 15112–15120
53. Lampard , C. *et al.* (1993) Tetrathiafulvalene as a catalyst for radical-polar crossover reactions. *J. Chem. Soc. Chem. Commun.* 3, 295–297
54. Pitzer, L. *et al.* (2019) Reductive radical-polar crossover: traditional electrophiles in modern radical reactions. *Chem. Sci.* 10, 8285–8291
55. Kischkewitz, M. *et al.* (2020) Radical-induced 1, 2-migrations of boron ate complexes. *Adv. Synth. Catal.* 362, 2077–2087
56. Xu, M. *et al.* (2025) Mechanism switch between radical-polar crossover and radical buffering. *Angew. Chem. Int. Ed.* 64, e202500522
57. Zhang, T. *et al.* (2025) Photoredox Fe-catalyzed aminoalkylation toward sterically hindered chiral β-amino acids. *J. Am. Chem. Soc.* 147, 37565–37575
58. Gould, C.A. *et al.* (2023) Rapid and modular access to quaternary carbons from tertiary alcohols via bimolecular homolytic substitution. *J. Am. Chem. Soc.* 145, 16330–16336
59. Pace, A.L. *et al.* (2024) Iron-catalyzed cross-electrophile coupling for the formation of all-carbon quaternary centers. *J. Am. Chem. Soc.* 146, 32925–32932
60. Gan, X.-C. *et al.* (2024) Carbon quaternization of redox active esters and olefins by decarboxylative coupling. *Science* 384, 113–118
61. Zhang, B. *et al.* (2022) Ni-electrocatalytic Csp^3–Csp^3 doubly decarboxylative coupling. *Nature* 606, 313–318
62. Tsymbal, A.V. *et al.* (2022) Nickel catalysis via S_H2 homolytic substitution: the double decarboxylative cross-coupling of aliphatic acids. *J. Am. Chem. Soc.* 144, 21278–21286
63. Mao, E. and MacMillan, D.W.C. (2023) Late-stage C(sp^3)–H methylation of drug molecules. *J. Am. Chem. Soc.* 145, 2787–2793
64. Chen, R. *et al.* (2024) Alcohol-alcohol cross-coupling enabled by S_H2 radical sorting. *Science* 383, 1350–1357
65. Li, J. *et al.* (2024) Enantioselective alkylation of α-amino C(sp^3)–H bonds via photoredox and nickel catalysis. *Nat. Catal.* 7, 889–899
66. Li, T. *et al.* (2025) Enantioselective alkyl–acyl radical cross-coupling enabled by metallaphotoredox catalysis. *J. Am. Chem. Soc.* 147, 10999–11009
67. Zhang, L.-L. *et al.* (2025) Enantioselective radical–radical cross-couplings of β-hydroxy amides and *N*-hydroxyphthalimide esters via Ni/photoredox catalysis. *J. Am. Chem. Soc.* 147, 33097–33107
68. Liu, W. *et al.* (2021) A biomimetic S_H2 cross-coupling mechanism for quaternary sp^3-carbon formation. *Science* 374, 1258–1263
69. Simoes, J.A.M. and Beauchamp, J.L. (1990) Transition metal-hydrogen and metal-carbon bond strengths: the keys to catalysis. *Chem. Rev.* 90, 629–688
70. Wang, Y. and Begley, T.P. (2020) Mechanistic studies on CysS – a vitamin B_{12}-dependent radical SAM methyltransferase involved in the biosynthesis of the *tert*-butyl group of cystobactamid. *J. Am. Chem. Soc.* 142, 9944–9954
71. Li, L.-J. *et al.* (2024) Enantioselective construction of quaternary stereocenters via cooperative photoredox/Fe/chiral primary amine triple catalysis. *J. Am. Chem. Soc.* 146, 9404–9412
72. Jia, Z. *et al.* (2022) Asymmetric C–H dehydrogenative allylic alkylation by ternary photoredox-cobalt-chiral primary amine catalysis under visible light. *J. Am. Chem. Soc.* 144, 10705–10710
73. Li, L.-J. *et al.* (2025) Acyclic quaternary stereocenters via catalytic asymmetric cross-couplings with unactivated alkyl *N*-hydroxyphthalimide esters. *Angew. Chem. Int. Ed.* 64, e202506883

74. Cui, X. *et al.* (2011) Enantioselective cyclopropenation of alkynes with acceptor/acceptor-substituted diazo reagents via Co(II)-based metalloradical catalysis. *J. Am. Chem. Soc.* 133, 3304–3307
75. Lu, H. and Zhang, X.P. (2011) Catalytic C–H functionalization by metalloporphyrins: recent development and future directions. *Chem. Soc. Rev.* 40, 1899–1909
76. Lee, W.-C.-C. and Zhang, X.P. (2024) Metalloradical catalysis: general approach for controlling reactivity and selectivity of homolytic radical reactions. *Angew. Chem. Int. Ed.* 63, e202320243
77. Lee, W.-C.-C. *et al.* (2023) Iron(III)-based metalloradical catalysis for asymmetric cyclopropanation via a stepwise radical mechanism. *Nat. Chem.* 15, 1569–1580